Environ Geol (2007) 51: 1157–1164
DOI 10.1007/s00254-006-0406-y

ORIGINAL ARTICLE

Qi Li
Zhishen Wu
Xing-lin Lei
Yutaka Murakami
Takashi Satoh

Experimental and numerical study on the fracture of rocks during injection of CO_2-saturated water

Received: 19 January 2006
Accepted: 13 June 2006
Published online: 22 August 2006

Q. Li (✉) · X. Lei · T. Satoh
Institute of Geology and Geoinformation, National Institute of Advanced Industrial Science and Technology, Tsukuba Central 7, 1-1-1 Higashi, Tsukuba 305-8567, Japan
E-mail: qi.li@aist.go.jp
Tel.: +81-298-613727
Fax: +81-298-613788

Z. Wu
Department of Urban and Civil Engineering, Ibaraki University, Nakanarusawa-cho 4-12-1, Hitachi 316-8511, Japan

Y. Murakami
Geological Survey of Japan, National Institute of Advanced Industrial Science and Technology, Tsukuba Central 7, 1-1-1 Higashi, Tsukuba 305-8567, Japan

Abstract Geological sequestration of CO_2 into depleted hydrocarbon reserviors or saline aquifers presents the enormous potential to reduce greenhouse gas emission from fossil fuels. However, it may give rise to a complicated coupling physical and chemical process. One of the processes is the hydro-mechanical impact of CO_2 injection. During the injection project, the increase of pore pressures of storing formations can induce the instability, which finally results in a catastrophic failure of disposal sites. This paper focuses mainly on the role of CO_2-saturated water in the fracturing behavior of rocks. To investigate how much the dissolved CO_2 can influence the pore pressure change of rocks, acoustic emission (AE) experiments were performed on sandstone and granite samples under triaxial conditions. The main innovation of this paper is to propose a time dependent porosity method to simulate the abrupt failure process, which is observed in the laboratory and induced by the pore pressure change due to the volume dilatancy of rocks, using a finite element scheme associated with two-phase characteristics. The results successfully explained the phenomena obtained in the physical experiments.

Keywords CO_2 · Geological sequestration · Dilatancy hardening · Two-phase medium · Two-phase flow · Fracture · Sandstone · Granite · Acoustic emission · Pore pressure

Introduction

Geological sequestration is an effective option for reducing CO_2 emissions to avoid the fast change of global warming. However, several key challenges should be faced before it is feasible. Low-cost technologies for securing CO_2 at coal-fired power plants and greater experience with CO_2 injection to avoid leakage to the surface are crucial to the success of large-scale CO_2 capture and disposal projects (Socolow 2005). Especially with the ratification of Kyoto Protocol in 2005, renovation plans of geological sequestration of CO_2 become more urgent than before. For a conceptual drawing of a typical geological sequestration system of CO_2 see Fig. 1. In practical processing, the captured CO_2 from large-scale point sources is transported and injected into deep reservoirs, such as saline aquifers, depleted oil and gas formations, depleted coal beds, etc. (Li et al. 2002).

Fracturing experiments were performed on sandstone and granite samples under triaxial conditions to investigate the role of CO_2-saturated water in the fracturing behavior of rocks. From the laboratory studies, the rock sample behaves as a progressive rupture process from the nucleation to crack failure with the increase of axial stress during the triaxial compressive experiments

(Lei et al. 2000), but the rock samples behave as an abrupt failure when keeping a certain level of the axial stress during the triaxial compressive experiments with injection of the CO_2-saturated water (Lei et al. 2003). From experiments, the rock failure induced by injection of water and/or CO_2 mainly results from the volume dilatant process. In this paper, the volume dilatant process observed in the experiments was simplified by a semi-empirical correlation and controlled by using a time dependent porosity technique. A multiphase finite element method is proposed to investigate the pore pressure change associated with the volume dilatancy in the laboratory. The influence of the CO_2-saturated water on the pore pressure change was examined during the volume dilatant process of rock samples. The computational results successfully explain the phenomena obtained in the physical experiment. The main result shows that CO_2-saturated water plays a key role in the acceleration of the dilatancy process of rocks. The dissipation of pore pressure is seriously controlled by the porosity magnitude of rocks.

Governing equations of transport of two-phase flow

The numerical simulation of a two-phase medium (solid and fluid) is necessary to account for geological sequestration problems of CO_2. The partial difference equations to be solved require the coupled solution of conservation of mass and momentum in the solid and the liquid phases, together with suitable boundary and initial conditions. Based on the fundamental concepts of the theory of porous media, the formulation of partial saturated flow problems may be derived from two-phase media formulation. The only primary state variable is pore pressures p. In the continuity equation, the term resulting from skeleton volume changes $\dot{\varepsilon}_{kk}$ should be neglected. Constitutive relation for the flow will obey the generalized Darcy law (Bear 1972).

The equilibrium equation of two-phase medium is expressed by

$$\sigma_{ij,j} + b_i = 0 \text{ in } \Omega \times T, \tag{1}$$

where b_i denotes body force. The constitutive equation is written by

$$\dot{\sigma}_{ij} = C_{ijkl}\dot{\varepsilon}_{kl}, \tag{2}$$

where C_{ijkl} is the fourth rank constitutive tensor. Analysis of the small strain tensor and the linear relation is assumed. The effective stress σ'_{ij} is given by

$$\sigma'_{ij} = \sigma_{ij} - Sp\delta_{ij}, \tag{3}$$

where S is the saturation coefficient.

Considering a simultaneous flow of two immiscible, incompressible fluids in rock porous media, i.e. a movement of a non-aqueous phase liquid through an initially wetting phase saturated porous media, a continuity equation for each fluid may be written as (Zhang 2001)

$$\phi(\mathbf{x})\frac{\partial S_i(\mathbf{x},t)}{\partial t} + \nabla \cdot \mathbf{q}_i(\mathbf{x},t) = 0, \tag{4}$$

where φ denotes the porosity, S_i is the saturation of fluid i, $i = 1$ or 2 standing for fluid 1 or 2, and $\mathbf{q}_i$ is the flux of fluid i.

Darcy's law can be extended to multiphase flow by considering a momentum balance for each phase of interest. Herein, the flux $\mathbf{q}_i$ is given by the two-phase extension of single-phase Darcy's law,

$$\mathbf{q}_i = -\lambda_i[\nabla P_i(\mathbf{x},t) + \rho_i\mathbf{g}], \tag{5}$$

where P_i is the pressure of fluid i, ρ is its density, $\mathbf{g}$ is the gravitational vector, and λ_i is the phase mobility of fluid i,

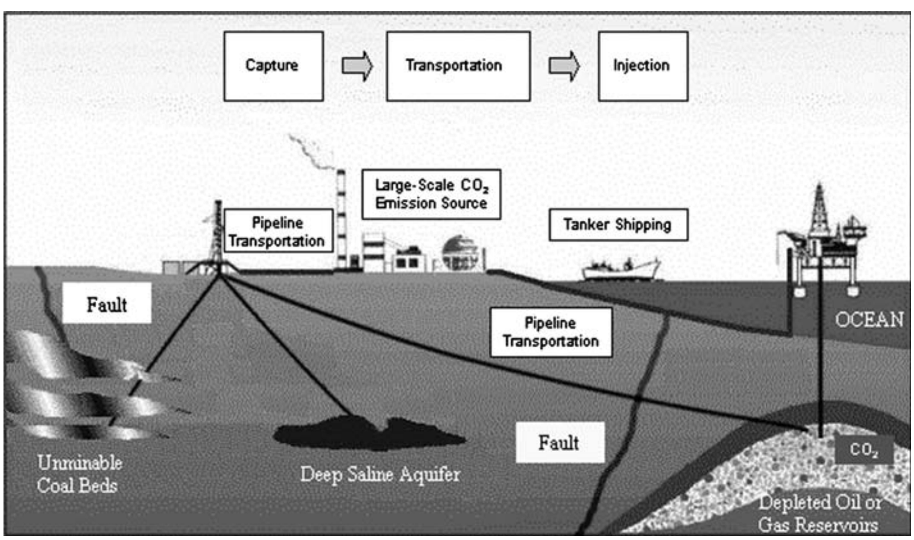

Fig. 1 A conceptual drawing of geological sequestration of CO_2

$$\lambda_i = k(\mathbf{x}) \frac{k_{ri}(S_i)}{\mu_i}, \tag{6}$$

where $k(\mathbf{x})$ is the intrinsic (absolute) permeability, k_{ri} is the phase relative permeability of fluid i, and μ_i is the phase viscosity of fluid i.

Substituting Eq. 5 into Eq. 4, the governing equations may be written in terms of the pressures in each of the two phases subject to appropriate boundary and initial conditions,

$$\phi(\mathbf{x}) \frac{\partial S_w(\mathbf{x}, t)}{\partial t} - \nabla \cdot \{\lambda_{\mathrm{w}}(\mathbf{x}, t)[\nabla P_{\mathrm{w}}(\mathbf{x}, t) + \rho_{\mathrm{w}} \mathbf{g}]\} = \mathbf{0}, \tag{7}$$

$$\phi(\mathbf{x}) \frac{\partial S_{\mathrm{nw}}(\mathbf{x}, t)}{\partial t} - \nabla \cdot \{\lambda_{\mathrm{nw}}(\mathbf{x}, t)[\nabla P_{\mathrm{nw}}(\mathbf{x}, t) + \rho_{\mathrm{nw}} \mathbf{g}]\} = \mathbf{0}, \tag{8}$$

where subscripts w and nw stand for wetting and nonwetting fluid phases, respectively. This is a typical mathematical system of two equations with four unknowns S_w, S_{nw}, P_w, and P_{nw}, and is usually linked by the relationships between saturation and capillary pressure,

$$S_{\mathrm{w}} + S_{\mathrm{nw}} = 1, \tag{9}$$

$$P_{\mathrm{nw}} - P_{\mathrm{w}} = P_{\mathrm{c}}, \tag{10}$$

where P_{c} is called the capillary pressure.

Rock experiments

Experiment description

Triaxial compressive experiments were conducted to investigate the behavior of rock samples under simulated geological sequestration conditions. In the triaxial experiments, cylinder samples of sandstone and granite were first loaded with a constant rate until dilatancy, or until the AE event from microcracking increased continuously (corresponding to some levels of 80–95% of fracturing stresses), and then the axial stress was kept constant. After that, the CO_2-saturated water was injected into the sample with a pressure of 5 MPa at a point when AE activity becomes stable. The confining pressure was kept constant at 20 MPa throughout each experiment. In the experiment, up to 32 piezoelectric transducer (PZT) sensors were mounted on the surface of the test sample to record the AE events. Confining oil was prevented from infiltration into the rock sample by encapsulation in silicone of 3–5 mm thickness. The photograph of the rock sample with mounted PZT sensors is shown in Fig. 2.

AE recording system

A rapid AE monitoring system was used to record the failure events in the rock samples. A technical drawing of the experimental set-up along with important details of the loading and AE recording systems is depicted in Fig. 3. The main advantages of the developed AE recording system are as follows: (1) The system has a fast waveform recording facility on 32 channels with a selection of sampling rate up to 25 MHz and dynamic range of 12 bits. (2) The mask time of the system is < 200 μs, thus making it possible to record AE waveforms without any important loss, particularly when the AE activity is very high, on the order of a few thousand events per second. (Any waveform recording system has a mask time for transmission of data after a trigger signal is detected. The system is in a frozen state and thus cannot record any new signal during the period of the data transmission.) (3) The system has a two-channel detector to capture the values of peak amplitudes up to the 99 dB dynamic range. As the noise level after passing through a 20 dB preamplifier is generally around 45 dB, the effective dynamic range for AE signal is 55 dB, which corresponds to a magnitude range of ~ 2.75. Further, as the peak detector shares a common base clock with the wave-form recording system, it is possible to obtain a complete set of temporal and spatial distributions of AE events (Satoh and Nishizawa 1997; Lei et al. 2000).

Fig. 2 Photograph of rock sample with mounted PZT sensors

In the experiment, the signal is pre-amplified by 40 dB before feeding into a fast waveform recording system which has a maximum sampling rate of up to 40 ns and a dynamic range of 12 bits. A two-channel peak detector was used to capture the values of the peak amplitudes after 20 dB pre-amplifiers. An automatic switch box was used for switching some sensors between AE measurement and velocity detecting during the experiment. Stress, strain, and confining pressure were recorded using two 16-bit analog to digital (A/D) boards.

Numerical simulations

Definition of computational domain

The geometry of specimens is shown in the axisymmetric cross section of Fig. 4. The finite element mesh is shown in the right of Fig. 4. The quadratic elements were used in the axisymmetric simulation. Rock samples are saturated with CO_2-saturated water under a certain differential pressure (Fig. 4). The simulation starts on a hydrostatic condition. The outer boundary of the cylinder specimen is impermeable.

Time dependent porosity

As observed from rock experiments, the volume dilatancy results in the increase of porosity of rock at a moment, especially of the dilatant core. To simulate such abrupt failure due to the pore pressure change induced by the volume dilatancy, a semi-empirical and easy-to-accomplish technique is proposed. The porosity sharply changes from the initial value to the double at time 20 min after the experiment starts. This change lasts 1 min according to a piecewise linear relationship (Fig. 5).

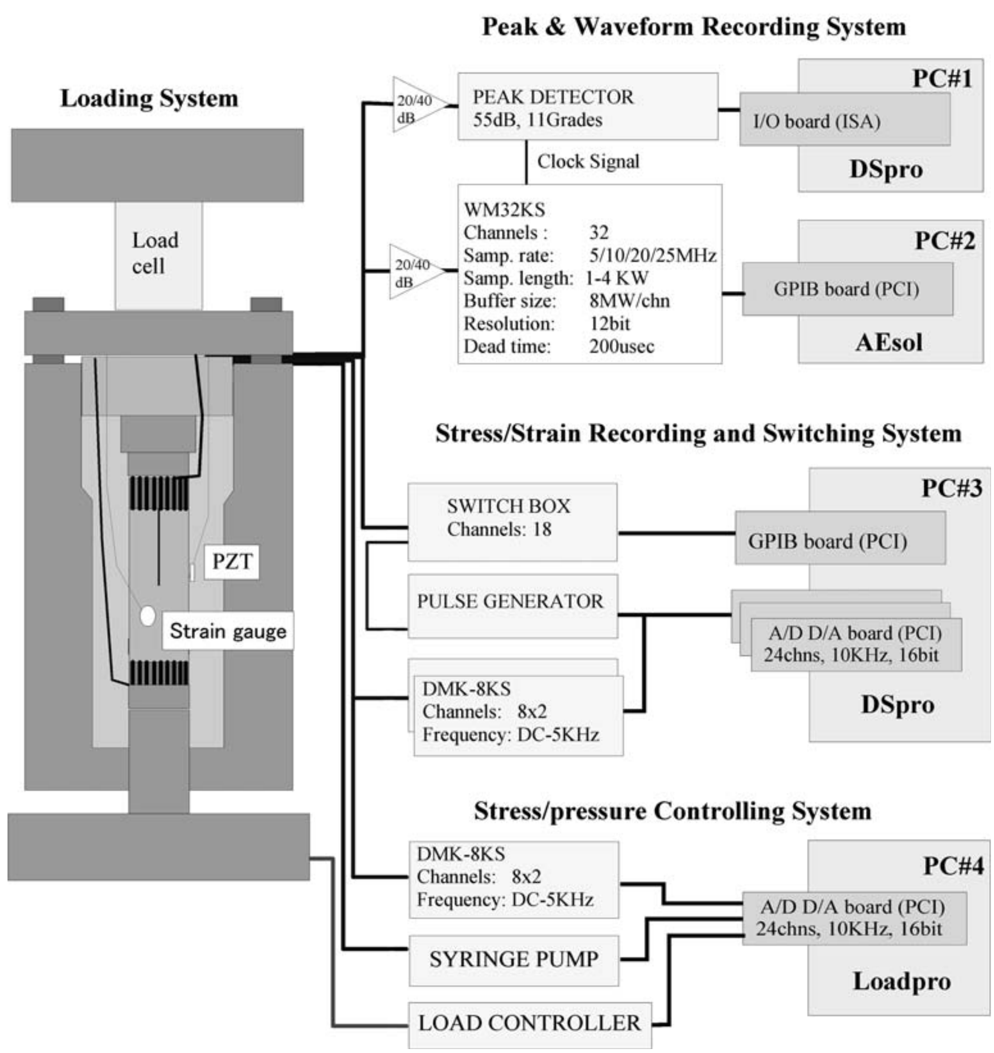

Fig. 3 A block diagram of the experimental system

Properties of rocks

Material parameters of two-phase media of the sandstone and granite samples are listed in Tables 1 and 2, respectively. The chosen values are mainly referred to chronological scientific tables 2005. The values are given according to statistical results of primary rocks in Japan (National Astronomical Observatory 2004).

Multiphase characteristic

The phase change relationship that determines S is based on the Clapeyron relation. In the past research, several methods have been proposed for computing the phase change. The most classical option, van Genuchten formulation, is adopted herein and plotted in Fig. 6 (Genuchten 1980).

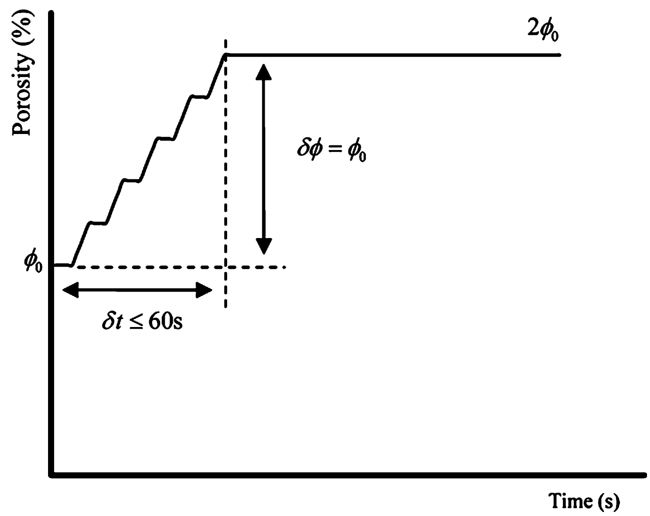

Fig. 5 Increase mode of time dependent porosity

Results and discussion

Experimental results

A typical experiment result of sandstone sample under CO_2-saturated water conditions is shown in Fig. 7. Experimental results show that CO_2-saturated water plays a central role in the fracturing process. A very strong positive feedback exists between fracture growth and fluid (water and CO_2) mitigation, suggesting an acceleration of fracture by increase of fluid permeability by cracking. The fracture nucleation process is strongly accelerated by CO_2-saturated water and thus results in an unpredictable catastrophic fracture.

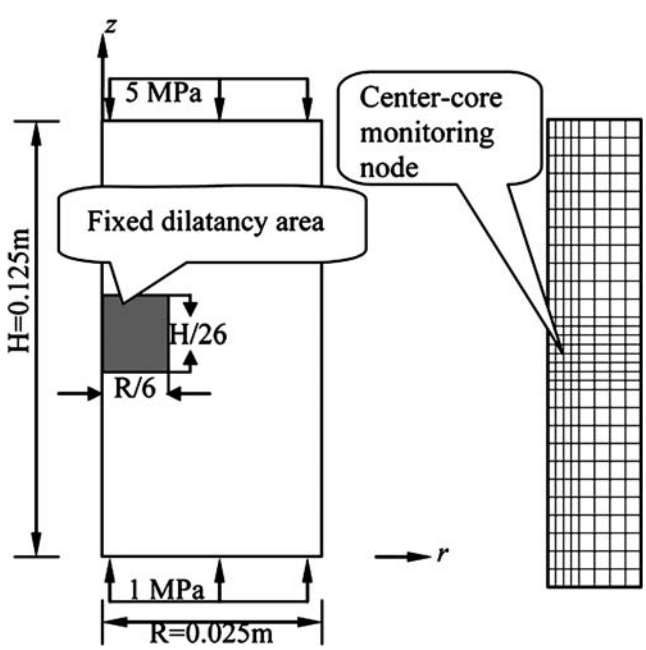

Fig. 4 Axisymmetric model (*left*) and finite element mesh (*right*)

Abrupt change of pore pressure

Figure 8 presents the pore pressure change at center-core monitoring node of sandstone samples. It shows that the existence of dissolved CO_2 in the rock changes the pore pressure faster than the existence of pure water during the dilatancy process. The solid line denotes the sandstone sample under pure water saturation, and the dash dot line denotes under CO_2 dissolved water saturation in the experiments. The fast increase of the pore pressure of the sandstone sample with CO_2-saturation just after the volume dilatancy may be interpreted for the abrupt failure of specimens in the triaxial, high pressure compressive experiments. The cumulative AE event counts and volumetric strain verify such an abrupt change of the pore pressure. Further comprehensive research is needed to interpret the intrinsic relationship between the volume dilatancy and the CO_2 solution.

Figure 9 presents the pore pressure change at center-core monitoring node of sandstone samples and granite samples under the same test conditions. The pore pressure change of the granite sample behaved slower than one of the sandstone sample. The reason can be explained by the compact physical property of the granite, i.e. the very lower porosity, which delays the dissipation of pore pressure during the dilatancy process. It shows that close-grained granite takes a longer time to return the initial pore pressure level after the drop resulted from the volume dilatancy. This is the case of dilatancy hardening. Sandstone as a typical rock of storage formations presents the merit rather than

Table 1 Material properties of solid media

Rock sample	Elastic modulus (Pa)	Poisson's ratio (–)	Density (kg/m^3)	Porosity (%)
Sandstone	5.0E + 09	0.25	2,660	6.20
Granite	7.0E + 11	0.15	2,580	2.00

Table 2 Material properties of fluid media

Rock sample	X-Permeability (m/s)	Y-Permeability (m/s)	Density of water (kg/m^3)	Density of CO_2 (kg/m^3)
Sandstone	3.0E–08	3.0E–08	1,000	1,800
Granite	1.0E–11	1.0E–11	1,000	1,800

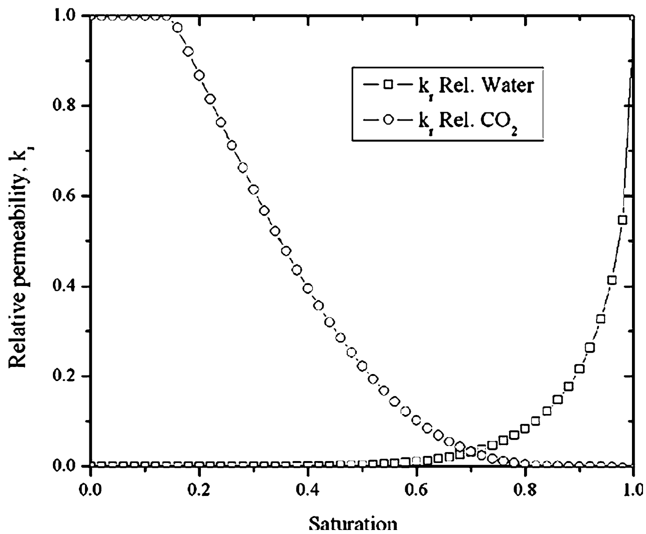

Fig. 6 Saturation versus relative permeability

granite. It hardly causes the dilatancy hardening, especially the existence of dissolved CO_2 further blocks the possibility of the dilatancy hardening. The well porosity of sandstone probably increases the total disposal amount of CO_2 in practice. However, the fast dissipation of pore pressure of sandstone results in the quick drop of

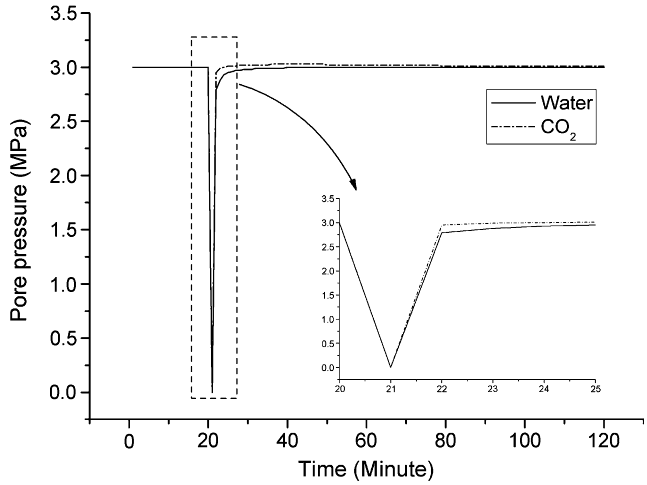

Fig. 8 Pore pressure change at center-core monitoring node for sandstone sample under water or CO_2 saturation

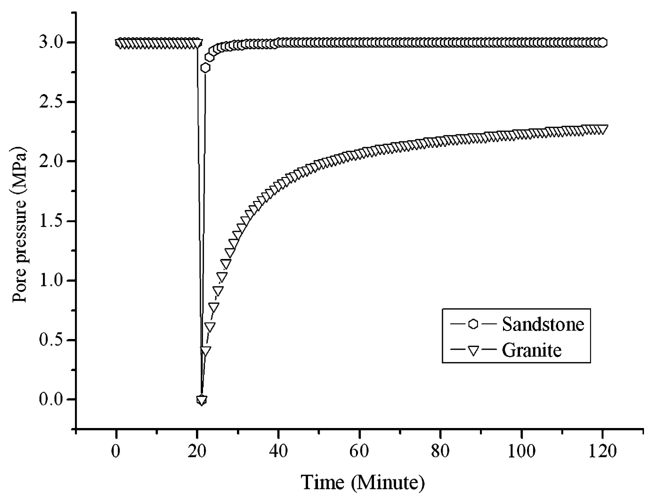

Fig. 9 Pore pressure change at center-core monitoring node of sandstone sample and granite sample

the effective stress, and this may trigger a catastrophic failure under certain extrinsic factors such as earthquakes. During choices of a practical disposal site, professionals should be aware of this point.

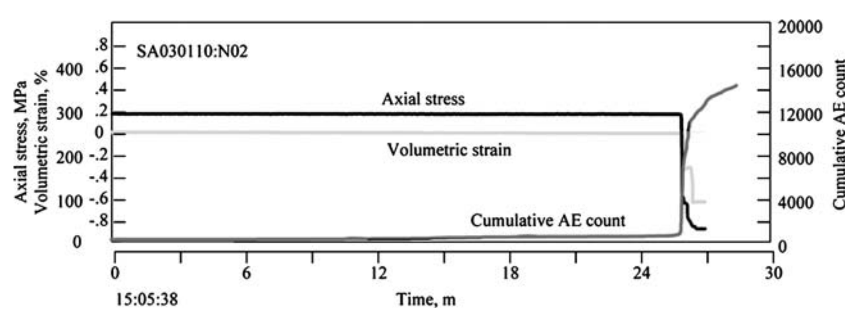

Fig. 7 Experiment result of sandstone sample

Distribution of pore pressure

Figures 10 and 11 show the contours of the pore pressure change of sandstone and granite samples at three typical stages, respectively. Pore pressure contours are plotted according to three stages, i.e. at initial stage (Time = 0 min), just after volume dilatancy (Time = 22 min), at stable stage (Time = 60 min). It

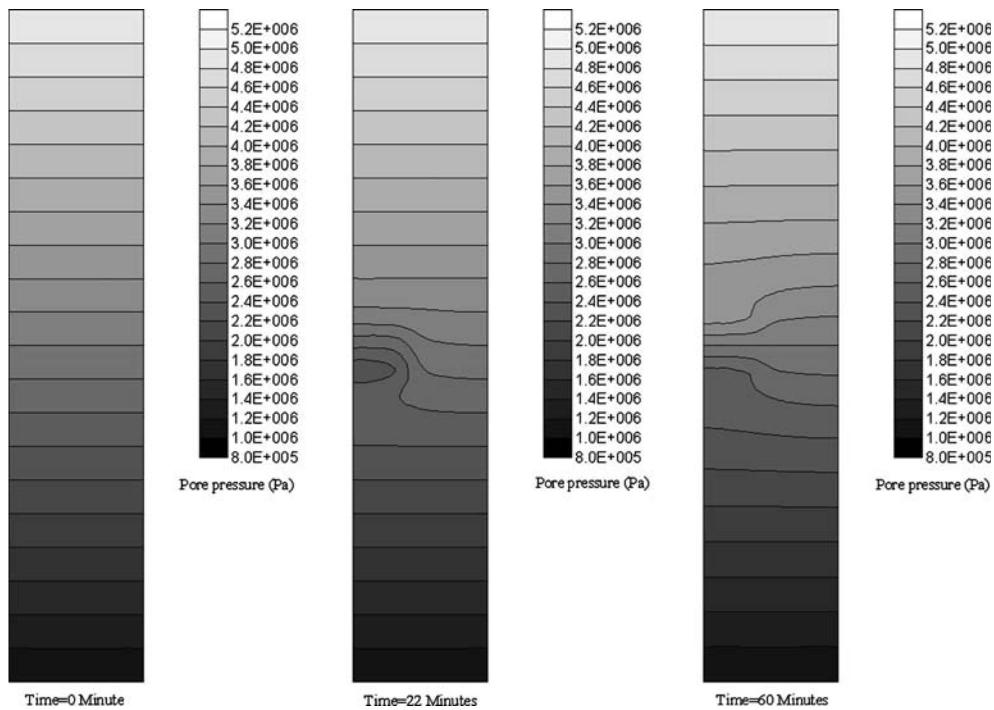

Fig. 10 Pore pressure contours of sandstone sample at initial stage (Time = 0 min), just after volume dilatancy (Time = 22 min), at stable stage (Time = 60 min)

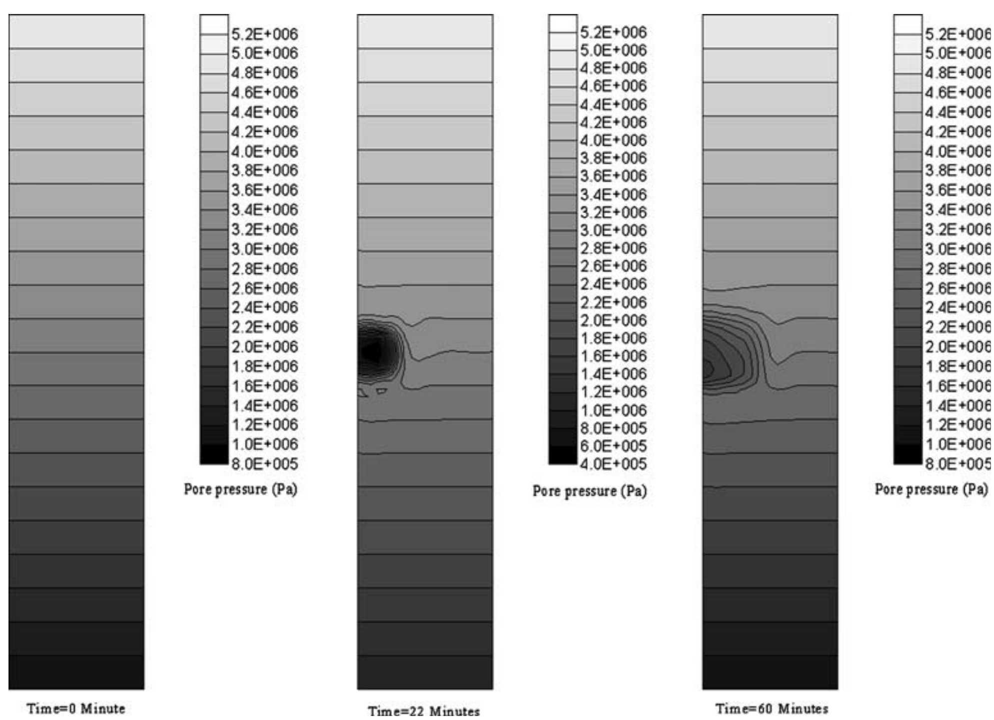

Fig. 11 Pore pressure contours of granite sample at initial stage (Time = 0 min), just after volume dilatancy (Time = 22 min), at stable stage (Time = 60 min)

presents a clear image of the pore pressure drop at the central fixed dilatancy part of rock samples. A long time period is needed to return the initial pore pressure level of granite after the drop resulted from the volume dilatancy. This is a typical case of dilatancy hardening. Although the good porosity of sandstone potentially increases the total sequestration amount of CO_2 in practice, the fast dissipation of pore pressure of sandstone results in the quick drop of the effective stress, and it hardly causes the dilatancy hardening. This point should be aware during the practice of geological sequestration.

Conclusions

A triaxial AE experiment was successfully conducted to monitor the abrupt failure of rock samples saturated with CO_2-saturated water simulating certain conditions of geological sequestration of CO_2. A two-phase numerical scheme is developed to validate the accelerating failure process due to phase change of CO_2. A time dependent porosity method is proposed to explain the pore pressure change due to the volume dilatancy. The numerical results successfully explain the phenomena obtained in the physical experiments. The existence of dissolved CO_2 clearly increased the pore pressure in rock samples during the volume dilatancy process. The quick dissipation of pore pressure of sandstone results in the quick drop of the effective stress, and this may trigger a catastrophic failure under certain extrinsic factors such as earthquakes. Professionals should be aware of this point during choices of a practical disposal site. This study is important not only concerning artificial reservoir problems such as CO_2 geological sequestration or underground oil storage but also for researches of natural earthquake processes.

Acknowledgment This work was partially supported by the Joint Earthquake Science Foundation of China under Contract No.104146.

References

Bear J (1972) Dynamics of fluids in porous media. Dover, New York

Genuchten V (1980) A closed form of the equation for predicting the hydraulic conductivity of unsaturated soils. Soil Sci Am Soc 44:892–898

Lei XL, Kusunose K, Rao MVMS, Nishizawa O, Satoh T (2000) Quasi-static fault growth and cracking in homogeneous brittle rock under triaxial compression using acoustic emission monitoring. J Geophys Res 105(B3):6127–6139

Lei XL, Nishizawa O, Xue Z (2003) Experimental study on the fractures of sandstone and andesite during injection of CO_2-saturated water by monitoring acoustic emission and velocity. Abstracts of EGS-AGU-EUG Joint Assembly 2003, Nice, France

Li Q, Wu ZS, Li XC, Ohsumi T, Koide H (2002) Numerical simulation on crust deformation due to CO_2 sequestration in deep aquifers. J Appl Mech (JSCE) 5:591–600

National Astronomical Observatory (2004) Rika Nenpyo (Chronological Scientific Tables 2005). Maruzen Co. Ltd., Tokyo

Satoh T, Nishizawa O (1997) A high speed, multi-channel waveform recording system for AE measurement (in Japanese with English abstract). Bull Geol Surv Jpn 48:439–446

Socolow RH (2005) Can we bury global warming? Sci Am 293(1):49–55

Zhang DX (2001) Stochastic methods for flow in porous media: coping with uncertainties. Academic, London